Available online at www.sciencedirect.com
SCIENCE DIRECT®
Journal of Power Sources 139 (2005) 356–365
JOURNAL OF POWER SOURCES
www.elsevier.com/locate/jpowsour

Retained molten salt electrolytes in thermal batteries

Patrick Masset[a,b,c,*], Serge Schoeffert[b], Jean-Yves Poinso[a,1], Jean-Claude Poignet[c]

[a] *Commissariat à l'Energie Atomique, Centre d'Etude du Ripault, BP 16, 37260 Monts, France*
[b] *ASB – Aerospatiale Batteries, Allée Sainte Hélène, 18021 Bourges, France*
[c] *Laboratoire d'Electrochimie et de Physicochimie des Matériaux et Interfaces, Ecole Nationale Supérieure d'Electrochimie et d'Electrométallurgie de Grenoble, Institut National Polytechnique de Grenoble, 1130 rue de la Piscine, BP 75, 38402 Saint Martin d'Hères, France*

Received 17 June 2004; accepted 10 July 2004
Available online 8 September 2004

Abstract

In high temperature electrical generators such as thermal batteries, the molten salt electrolyte needs to be retained by a binder, e.g. MgO. We have pointed out that the magnesia volume fraction was a more accurate parameter than the usually used weight fraction. Moreover, based on our technique measurements, we defined a magnesia volume fraction range (27–30 vol.%) where the electrolyte retention could be considered as efficient whatever its nature. And finally, we proposed a microstructure description of the retained electrolyte.

Keywords: Electrolyte; Retention; Thermal battery; MgO magnesia

1. Introduction

In thermal batteries, the electrolyte is in the solid state at room temperature. After thermal activation (pyrotechnic combustion), the electrolyte becomes liquid, and then conductive due to the ionic species motion between the anode and the cathode. Molten salts are suitable media as electrolytes in thermal batteries. Due to high level of mechanical stresses (acceleration, gyration, etc.) during the operation time, the liquid electrolyte needs to be retained by a binder. By means of the capillary forces, the electrolyte is stabilized.

Few materials could be used as electrolyte binder. In the past, SiO_2 silica was widely used. Its use was abandoned because of its high reactivity with molten lithium at high temperature. Moreover, silica could react with molten fluoride based salts. Other metal oxides such as Y_2O_3, $LiAlO_2$, ... were envisaged as the electrolyte binder [1]. We may mention that the BN boron nitride was also used. Finally, MgO was found the most efficient material in the replacement of silica. Its solubility in molten alkali halides is considered to be low enough. In the LiCl-KCl eutectic, the solubility product ($pK = [Mg^{2+}][O^{2-}]$) was found to be equal to 7.2 at 450 °C [2] and 8.38 at 700 °C [3]. From the thermodynamic point of view, magnesia is stable even with molten fluorides whatever the considered temperature this is opposite to silica. But a high weight fraction is required to obtain an efficient electrolyte retention.

The amount of the binder electrolyte is one the most important parameters. If the magnesia ratio is too low, short-circuits may occur

- between the anode and the cathode (no physical separation);
- by electrolyte leakage between two stacks.

In the both cases, the current and voltage of the battery cannot be reached in its operating time. The battery is considered to be destroyed.

* Corresponding author. Present address: European Commission, Joint Research Centre, Institute for Transuranium Elements, P.O. Box 2340, 76125 Karlsruhe, Germany. Tel.: +49 7247 951 152;
fax: +49 7247 951 593.
E-mail address: Patrick.Masset@itu.fzk.de (P. Masset).
[1] Present address: Commissariat à l'Energie Atomique, Centre de Valduc, 21120 Is-sur-Tille, France.

0378-7753/$ – see front matter © 2004 Elsevier B.V. All rights reserved.
doi:10.1016/j.jpowsour.2004.07.009

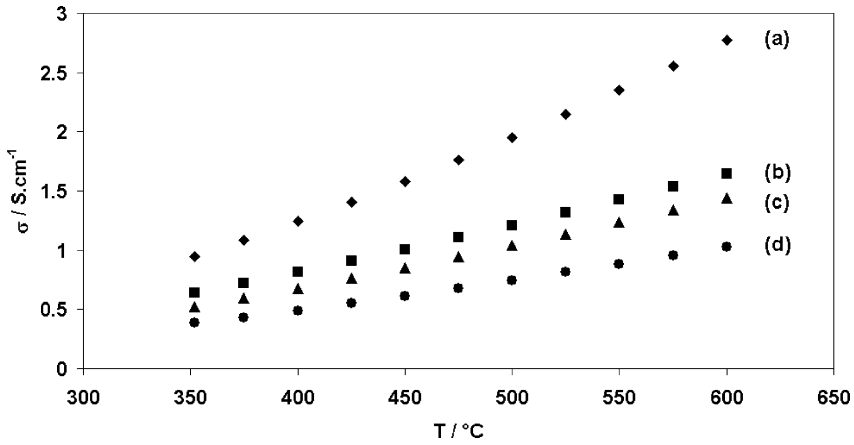

Fig. 1. Ionic conductivity σ (S cm^{-1}) of LiCl-KCl based separators vs. the temperature and the weight fraction of magnesia (MgO (a) 0%, (b) 35%, (c) 40%, (d) 50%).

However, if the magnesia ratio is too high, two consequences are expected:

- the separator deformation is insufficient to allow electrode wetting by the electrolyte, it induces an increase in the contact resistance;
- electrolyte binders are electrical insulators, so that the ionic conductivity decreases drastically with the amount of magnesia as sketched in Fig. 1 (data issued from reference [4]).

Finally, the overall resistance of the battery increases and the cell voltage decreases. To reach the electrical requirements, stacks could be added but the mass and the volume of the battery increase.

Numerous physical parameters influence electrolyte retention. The separator (electrolyte + binder) is obtained by electrolyte and magnesia powders compaction at room temperature. The density of the pellets could also occur. A much more appropriate amount of magnesia required in the separator was determined for some electrolytes. Data available are summarized in the Table 1.

Concerning the LiF-LiCl-LiI electrolyte, Guidotti and Reinhardt [5] used 35 wt.%. To our knowledge, this value was not optimized. This value was taken as a reference for the present study.

Recently, a new process was proposed [6]. It consists of a ceramic felt filled with electrolyte. Thinner and higher mechanical resistant separators were obtained than the usual process. But, magnesia-based separators are still industrially used and more studies are needed to have a better understanding.

The aim of the present work is to determine the appropriate amount of magnesia needed to obtain good electrolyte retention. Moreover, we expect to understand more precisely the retention phenomenon by observing separator microstructural features.

Table 1
Magnesia weight and volume fractions used in the separator [8]

	LiCl-KCl	LiCl-LiBr-KBr	LiF-LiBr-KBr	LiF-LiBr-LiCl
Ψ_{MgO} (wt.%)	40	30	25	35
Ψ_{MgO} (vol.%)	23.3	21.2	20.8	25.2

2. Experimental

2.1. Materials

2.1.1. Salts

LiF, LiCl, LiBr (99.99% purity) were supplied by Sigma–Aldrich. Lithium iodide of 99.9% purity (−200 mesh) was purchased from Cerac. They were used as starting materials. The salts were dried individually under vacuum in a quartz crucible during 15 h. The mixtures were fused under argon, in glassy carbon crucibles to prevent silica dissolution in the presence of fluoride ions, and maintained at 500 °C for 15 h. They were quenched directly in the grinder. Once ground, they were stored in a glove box under argon. Impurity concentrations (mainly oxides and hydroxides) were determined to be less than 10^{-4} molar fraction. In the case of LiI, a molar fraction of 5.10^{-2} was measured. Electrolyte compositions are reported in Table 2.

2.1.2. MgO magnesia

MgO powder, used as an electrolyte binder (E.B.), was provided by ASB – Aerospatiale Batteries. The MgO samples were slowly heated from room temperature to and maintained at 850 °C for 15 h in argon gas atmosphere.

Table 2
Melting point (mp), molar and weight compositions of the electrolytes used in this study

Electrolytes	mp (°C)	Composition (wt.%)	Composition (mol%)	References
LiF-LiCl-LiBr	443	9.6-22-68.4	22-31-47	[9]
LiF-LiCl-LiI	341	3.2-13-83.8	11.7-29.1-59.2	[10]
LiCl-KCl	354	44.8-55.2	58.8-41.2	[11]
LiI-KI	285	58.2-41.8	63.3-36.7	[12,13]

This was done to prevent hydration and carbonate formation.

2.1.3. Separator preparation

Appropriate amount of MgO and salt powders were accurately weighed and thoroughly mixed in a silica crucible to give about 50 g of the mixed powder in each case. The corresponding mixtures were fused during 15 h at 500 °C in vitreous carbon crucibles. As described previously for electrolytes, they were quenched directly in the grinder. After grinding, they were stored under argon atmosphere in a glove-box. The ground powders were pressed uniaxially into pellets of 35 mm in diameter and approximately 500 μm thickness.

For the SEM experiments, we used four LiCl-KCl (*x*% MgO) mixtures. The *x* value varied from 20 to 50% in steps of 10%. The pellets from each batch were placed in a vitreous carbon crucible and then heated for 15 h at 500 °C under argon atmosphere in a glove box. Afterwards, the pellets were quenched. They were fractured along the diameter. The cross-section was observed by means of SEM coupled with EDS analysis.

2.2. Techniques and apparatus

2.2.1. DTA/TGA analysis

Thermal analyses were performed using a Setaram 24 thermal analyzer equipped with a double oven (in order to increase the TGA sensivity and stability). Experiments were carried out in a dynamic atmosphere (flow rate of 1.25 l h^{-1}) of dry helium (less than 1 ppm H_2O) on 100 mg samples. We used 100 μl alumina Al_2O_3 crucibles. Samples were prepared in a glove box to prevent hydration.

We controlled the drying procedure and checked the electrolyte melting point.

2.2.2. X-ray diffraction (XRD)

X-ray diffraction patterns were obtained with a Siemens D500 diffractometer, using CoKα radiation (λ = 1.789 Å) equipped with a linear detector. X-ray diffraction was performed on samples protected by a polyethylene film to prevent a reaction with water.

2.2.3. Scanning electronic microscopy (SEM)

Microstructural features of the starting materials and the separator were determined by using a JEOL scanning electron microscope. Semi-quantitative compositional analyses in different region of the separator were carried out by energy dispersive analysis by X-rays (EDAX) on the EDS system attached to the JEOL scanning electron microscope. Microscopic images were collected both on powders and separator fractured surfaces to discern compositional changes. No thin films of gold on the exposed surfaces were applied before microscopic viewing. Samples were sufficiently electrical conductive and no electrostatic charging was noticed.

2.2.4. He pycnometry

MgO and salts powders densities were measured by means of a helium gas pycnometry technique. The apparatus was an automatic Accupyc 1330 supplied from Micrometrics. Preliminary samples were prepared in a glove box and transferred to the analysis chamber in a closed pan in order to prevent powder hydration. Experiments were repeated three times in order to estimate the error. Dispersion of the values was less than 0.5%. We give the average values.

2.2.5. Molten salt densities

We used a home made technique to measure the molten salt densities. We determined the volume occupied by the molten salt in a crucible designed for the purpose. We estimated the uncertainty to be less than 5% with the technique we used.

2.2.6. Separator deformation

Pellet-deformation tests were carried out with a modified technique described in the literature [7]. The deformation measurements consisted of a change in thickness of pellet under applied pressure. The deformation tests were carried out at 500 °C. During the test, the pellet was held between two mica sheets. Before the test deformation, the thickness of the separator and mica sheets were measured individually and together. A pressure was applied by means of a weight. All the apparatus was preheated at 500 °C for half an hour before each experiment. The pressure was applied for a quarter an hour and then the separator was quenched. The thickness change was determined by means of a micrometer. In the reference cited before, they measured deformation at high temperature. In our case, all the deformation measurements were done at room temperature. So that, our determinations might be slightly higher than the literature values.

3. Results and discussion

3.1. Starting materials characterization

3.1.1. Salts

First of all, we checked the correct composition of the prepared electrolytes by means of DTA/TGA analysis (weight variations and melting point). No significant weight losses in the 100–200 °C range corresponding to the alkali halides hydrates decomposition temperatures were noticed. Weight losses after the drying procedure were less than 0.1 wt.%. Thus, we were sure that the drying procedure we used was efficient. Concerning the electrolyte melting point, except the LiI-KI one, we noticed no discrepancies between our determinations and the literature values. The LiI-KI melting point was found to be close to 285 °C which agreed with the data of Johnson and co-workers [12]. Leiser and Whittemore [13] who proposed a value equal to 265 °C. We thought that water contamination could explain this difference.

The specific properties we needed in our study were the salt densities. The measurements were done at 25 and 500 °C

Table 3
Summary of the literature and experimental values of liquid salt densities ρ(l) at 500 °C and solid salt densities ρ(s) at 25 °C

Salts	ρ(s) (g cm^{-3})		ρ(l) (g cm^{-3})	
	Literature	Experimental	Literature	Experimental
LiCl-KCl	2.02[a]	2.01 (5)	1.6 [14]	1.59
LiI-KI	3.85[a]	3.53 (3)	2.77[b] [15]	2.83
LiF-LiCl-LiBr	2.92 [16]	2.91 (4)	2.19 [8]	2.17
LiF-LiCl-LiI	3.54[a]	3.51 (3)	–	2.69

[a] Calculated values.
[b] Values for rich-LiI-KI mixtures (80:20 mol%).

(it corresponds to the temperature at which we made deformation experiments). All the densities measured are reported in the Table 3.

We used the Eq. (1) to calculate mixture densities at room temperature when no data were available in the literature.

$$\rho = \left(\sum_i \frac{f_i^m}{\rho_i} \right)^{-1} \quad (1)$$

where f_i^m and ρ_i are respectively the weight fraction and the density of the ith compound.

We observed a good agreement between our data and the literature (or calculated values).

3.1.2. MgO magnesia

Preliminary, MgO powder was studied by means of X-ray diffraction and SEM coupled with EDS analysis. We checked that no other phases were present after the drying step (Fig. 2). Peaks were indexed using the JCPDS file number 04829. The crystallite size was obtained by using the Debye–Scherrer relation and the half-peak broadening.

Using the diffraction peak shape, we were able to determine the MgO crystallite size. It was found to be close to 45 nm.

By means of SEM technique, spherical MgO particle size was determined to be around 50 nm (Fig. 3). It agrees with the previous determination by XRD analysis. To complete magnesia characterization, its density was evaluated at room temperature. The data obtained are summarized in the Table 4.

3.2. Separator deformation measurements

The aim of these experiments was to define the optimum weight fraction of magnesia in separators for each electrolyte.

In the first part, we report deformation tests results and we consider the influence of the salt densities. In the second part, we propose a description of the microstructural feature changes in the separators at high temperature. Some interesting results were obtained by collecting SEM images of fractured separators.

Table 4
MgO magnesia properties

Parameters	Experimental values	Techniques
Particles size	50 nm	SEM
	45 nm	XRD
Density	3.39 g cm^{-3}	He pycnometry

3.2.1. Optimum MgO magnesia fraction

Deformation tests were carried out at 500 °C. The applied pressure was equal to 0.45 daN m^{-2}. Although, tests were realized in an quarter an hour, the main deformation appeared in the first 5 min. Deformation tests were driven with different magnesia weight fractions to evaluate the optimum value. It ranged between 20 and 50 wt.% depending the electrolyte nature.

For the binary electrolytes (LiI-KI and LiCl-KCl eutectics), we did not manage to obtain the curves representing the pellet thickness variations versus the magnesia weight fraction. We determined only the minimum amount of magnesia needed to retain efficiently the molten salt electrolytes. The corresponding MgO weight fraction values for LiI-KI and LiCl-KCl were respectively 35 and 45 wt.%. Below these values, the separators behaved as a viscous liquid. We were not able to provide an accurate measurement of the pellet deformation.

However, concerning the ternary electrolytes, were able to measure the pellet deformation with different amounts of magnesia (Fig. 4). One can observe that LiF-LiCl-LiBr based pellet deformation was twice that of the LiF-LiCl-LiI based pellet deformation.

As the weight fraction increases the pellet deformations decreases. MgO particle number by volume unity increases, thus capillary forces increase correlatively. Thus, we might expect that the volume fraction of magnesia would be a more significant parameter than the weight fraction.

To ensure the anode and the cathode wetting by the electrolyte contained in the separator, a deformation between 15 and 30% is required. We defined the optimum weight fraction of magnesia when the deformation pellets was around −20%. The corresponding values we determined are summarized in the Table 5.

3.2.2. Volume fraction: the pertinent parameter

In this part of the study, we demonstrate that the magnesia volume fraction is the parameter to be considered.

The volume fractions of magnesia ψ^v_{MgO} contained in the pellets were calculated using the Eq. (2).

$$\psi^v_{MgO} = \frac{\psi^w_{MgO}}{(\psi^w_{MgO}/\rho_{MgO}) + (1 - (\psi^w_{MgO}/\rho_{salt}))} \quad (2)$$

where $\psi^v_{MgO}$and ψ^w_{MgO} are respectively the volume and weight fractions of magnesia contained in the separator.

Table 5
Summary of the optimum volume and weight fractions of magnesia

	LiCl-KCl	LiF-LiBr-LiCl	LiI-KI	LiF-LiCl-LiI
Ψ_{MgO} (wt.%)	45	40	35	32.5
Ψ_{MgO} (vol.%)	27.2	29.4	30.3	27

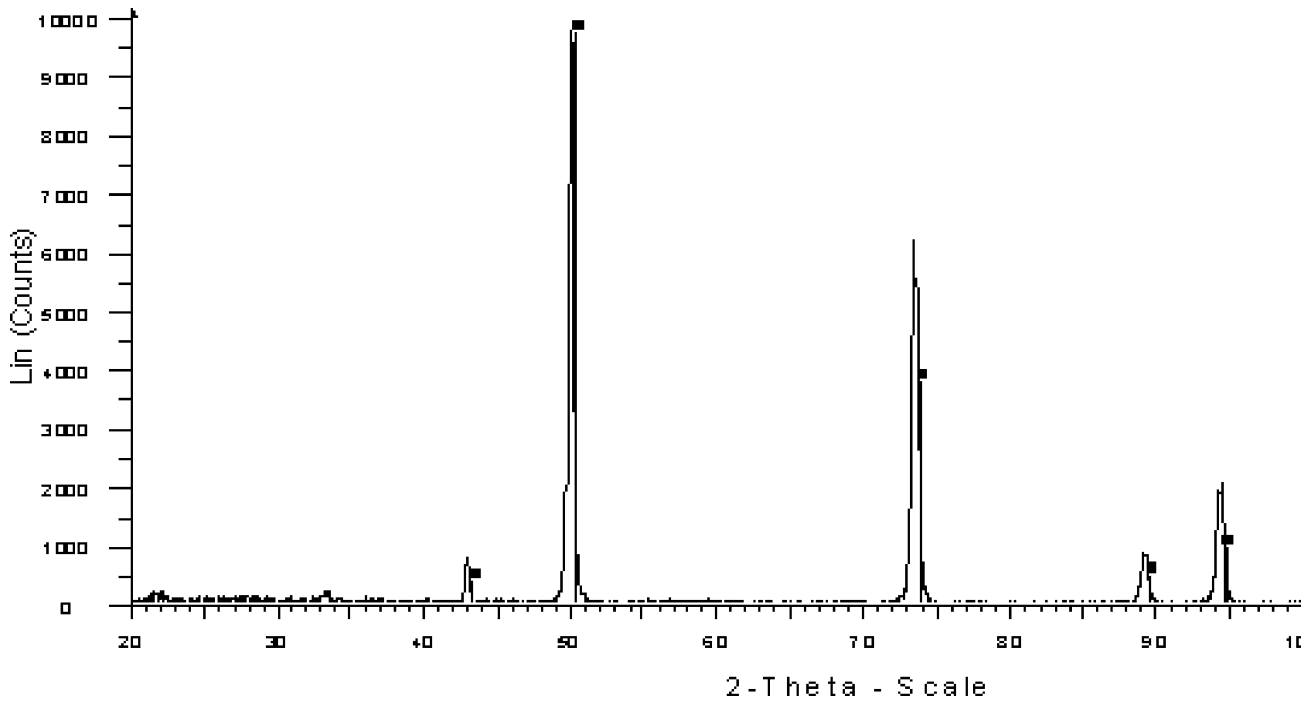

Fig. 2. X-ray diffraction pattern on MgO powder sample.

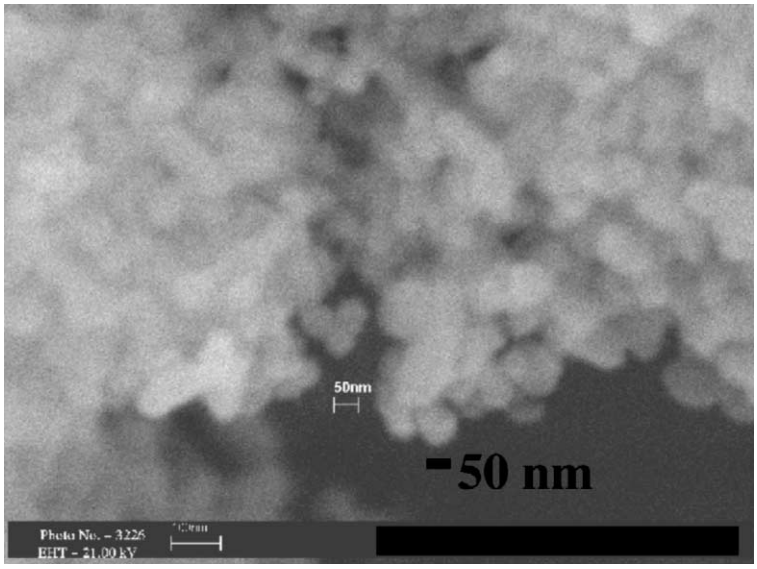

Fig. 3. MgO powder observed by SEM.

Considering the optimum magnesia weight fractions we determined or published in the literature, values ranged between 25 and 45%. Analyzing the driving forces involved in the retention phenomena, they were considered to be more linked to volume fraction than weight fraction.

We present a diagram (Fig. 5) which allow us to have a direct conversion between the weight and the volume fraction versus the molten salt densities.

We cannot compare directly our results with the published data because we did not use the same technique. Literature data (full markers) were centered on the value of 23 ± 2.2 vol.% whereas our data (empty markers) ranged from 27 to 30 vol.%. The first conclusion was that the optimum values ranged was within a small difference, less than ± 2 vol.%, instead of ±10 wt.%. Secondly, our values were 15% greater than literature one. Thus, a comparison could be made.

We showed that volume parameter was a more accurate parameter than weight fraction. Moreover, we defined a volume fraction range where electrolyte retention could be considered as efficient whatever the electrolyte nature. Finally, a value around 27–30% (or 23–25 vol.% with literature data) was found to be good.

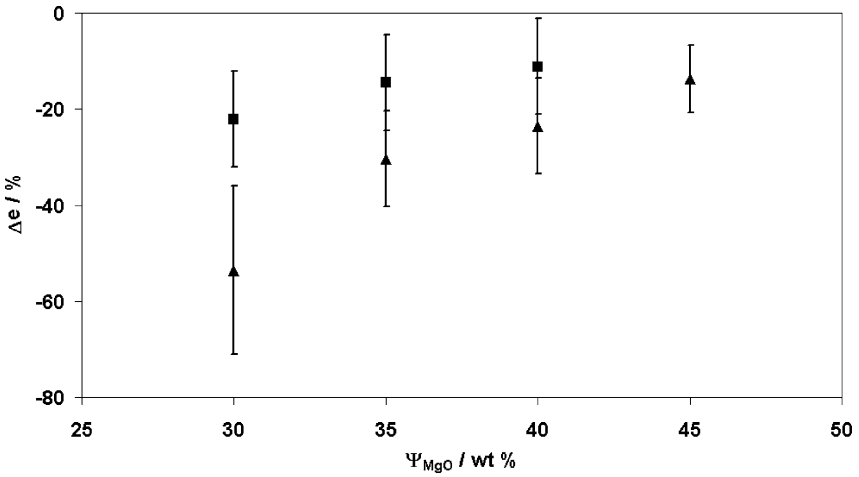

Fig. 4. Separator thickness variations $\Delta\varepsilon$ vs. the MgO weight fraction, (■) LiF-LiCl-LiI, (▲) LiF-LiCl-LiBr, T = 500 °C, P = 0.45 daN m^{-2}.

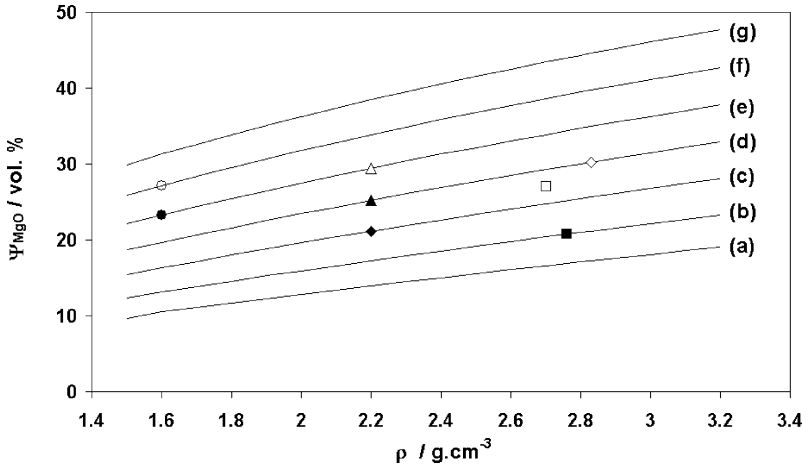

Fig. 5. Corresponding volume/weight conversion depending the salt densities and weight fractions: (a) 20%, (b) 25%, (c) 30%, (d) 35%, (e) 40%, (f) 45%, (h) 50%, salts: (●) LiCl-KCl [8], (■) LiF-LiBr-KBr [8], (▲) LiF-LiCl-LiBr [8], (♦) LiCl-LiBr-KBr [8], (△) LiF-LiCl-LiBr (this work), (◯) LiF-LiCl-LiI (this work), (◯) LiCl-KCl (this work), (◊) LiI-KI.

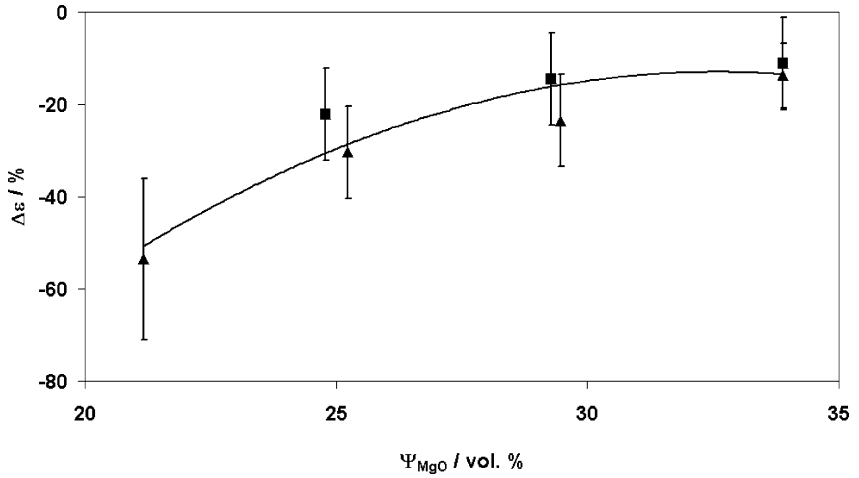

Fig. 6. Separator thickness variations $\Delta\varepsilon$ vs. the MgO volume fraction, (■) LiF-LiCl-LiI, (▲) LiF-LiCl-LiBr, T = 500 °C, P = 0.45 daN m^{-2}.

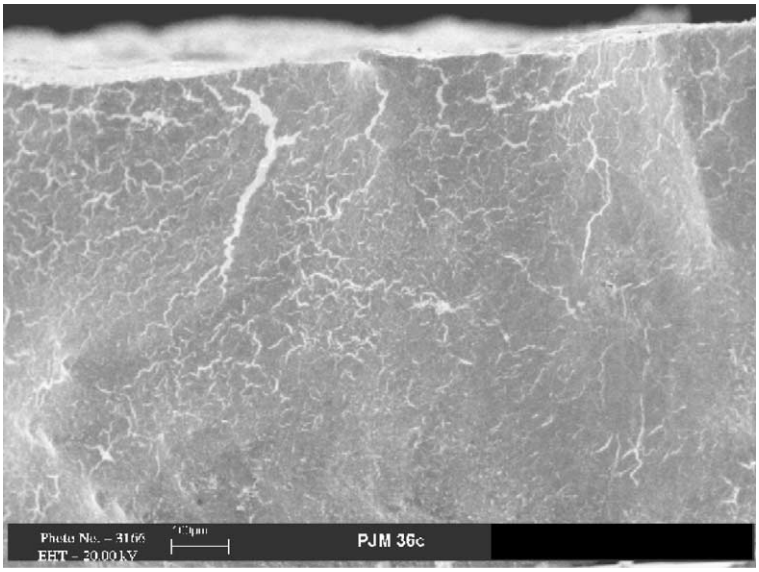

Fig. 7. SEM image collected on fractured surfaces of pellets, ψ_{MgO} (wt.%) = 20%.

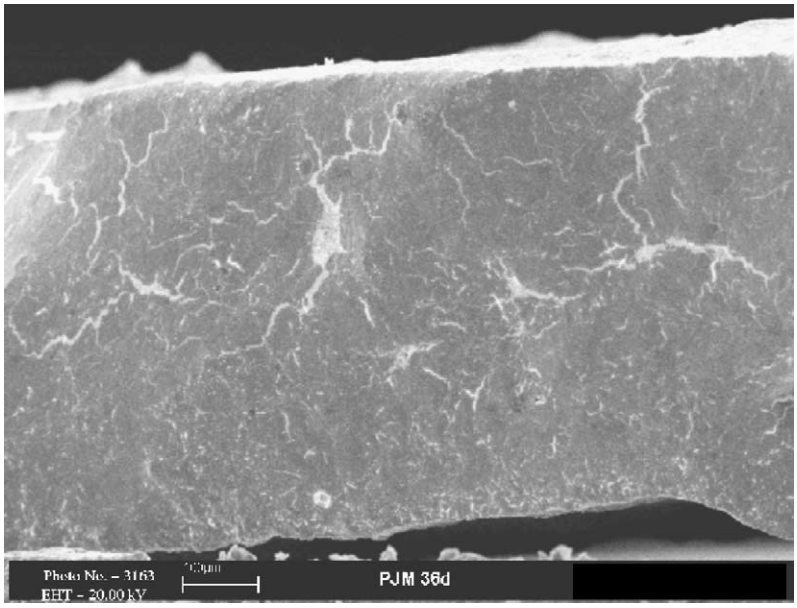

Fig. 8. SEM image collected on fractured surfaces of pellets, ψ_{MgO} (wt.%) = 30%.

We represented the curves thickness variations versus the volume fraction (Fig. 6). Experimental points were located on the same master curve. The optimum value was determined to be close to 28 vol.%. This value would be equivalent to 23.8 vol.% value determined by the technique described in the literature. It corresponds to the average value obtained by this technique.

3.3. Separator microstructural features

As a way to understand the mechanical behavior of pellets, we studied the microstructural evolution of heated pellets. We present images obtained by SEM of fractured pellets with different amounts of magnesia. Thus, insights were made on interesting parts of the fractured surface.

3.3.1. MgO magnesia proportion influence

We prepared LiCl-KCl (*x* wt.% MgO) pellets. The *x* values ranged between 20 and 50. They were heated at 500 °C for 15 h in an argon atmosphere. After quenching, fractured pellets were observed by means of scanning electron microscope (Figs. 7–9) coupled with EDAX analysis.

We observed two types of microstructural features. They were referenced as bulk (dark) and filamentous (gray). During the SEM observations, we made sure that the filaments could not be ascribed to surface effects (roughness, etc.).

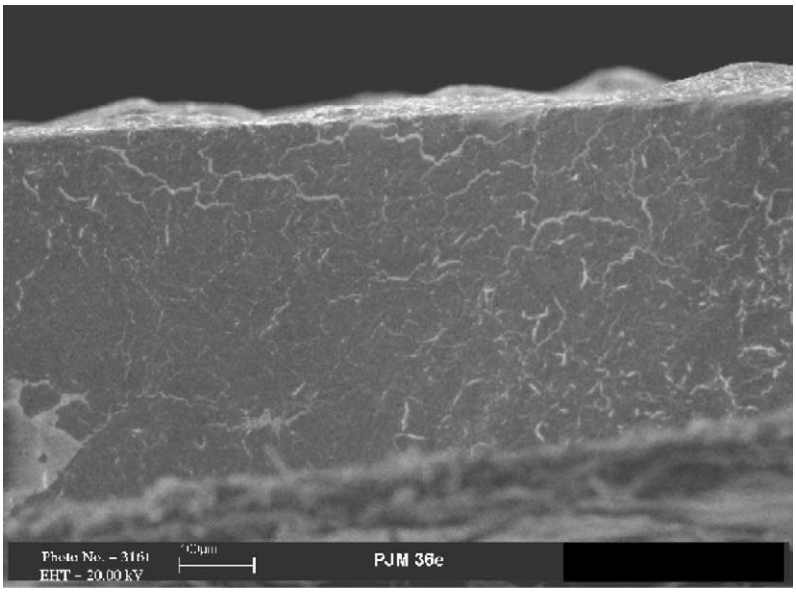

Fig. 9. SEM image collected on fractured surfaces of pellets, ψ_{MgO} (wt.%) = 40%.

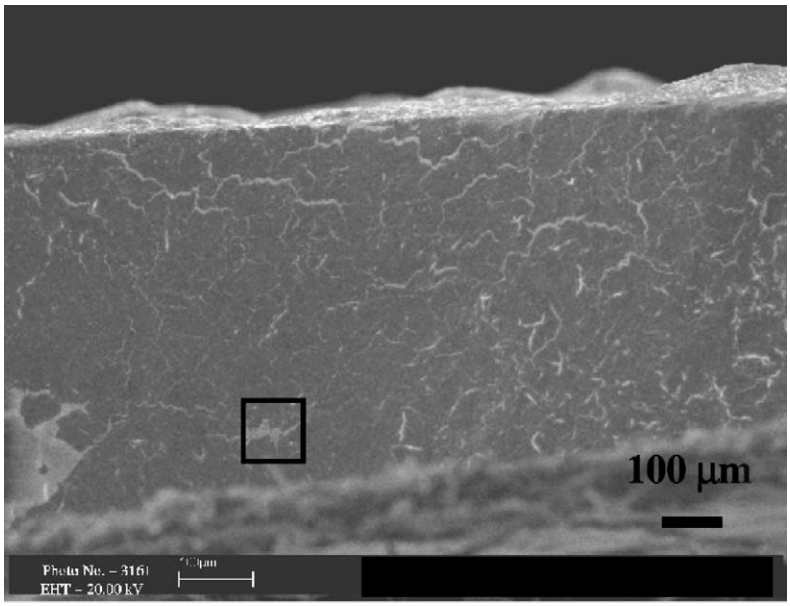

Fig. 10. SEM images collected on fractured surfaces of pellets containing 40 wt.% magnesia.

As the weight fraction of magnesia was increased, we observed correlatively that the number and the size of the filaments decreased. These observations led us to think that a three dimensional organization occurred during the heating of the pellets with the interconnection of the filaments. We characterized the filaments by coupled scanning electron microscopy and EDAX analysis to known more about the local structure of the observed filaments.

3.3.2. Insight on the separator structure

For each magnesia ratio, we carried out local observations of the filaments in different parts of the pellets. Our conclusions were the same whatever the magnesia ratio and the places we made the observations.

An example of the views we obtained by SEM technique is presented in the Fig. 10. We focused our observations on the gray filamentous areas. Details within the dark square in the Fig. 10 are magnified in the next picture Fig. 11 and so on with Figs. 12 and 13. We made comparative EDAX analysis in the dark and gray area of the pellets. The intensity corresponding to the Mg element was found be distinctly higher in the filament than the one in the matrix (Fig. 14). We suggest that the filaments were enriched magnesia area. These analyses were corroborated by the local observations of MgO particles (Fig. 13). We believe that a three dimensional structure may have occurred during the heating and a solid-like structure formed. The separator could be considered as a classical biphasic media. Thus, the short order organization appear-

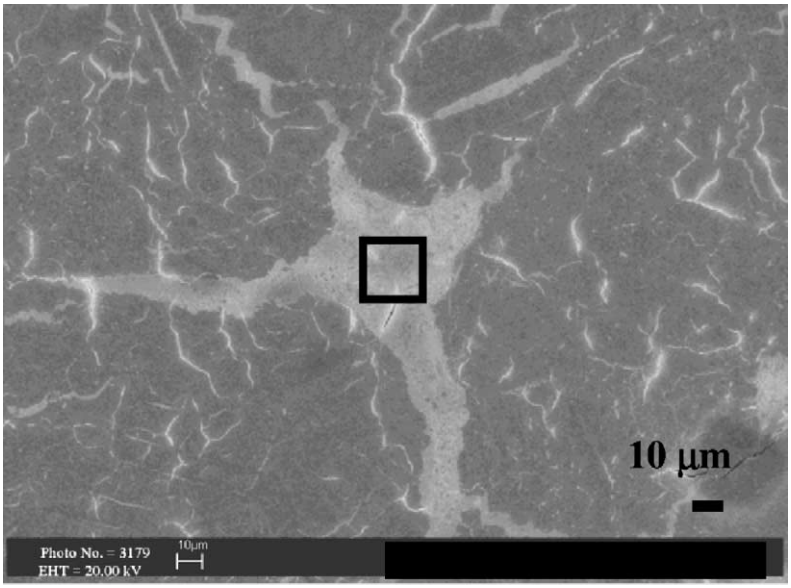

Fig. 11. SEM images collected on fractured surfaces of pellets containing 40 wt.% magnesia (detail of Fig. 10).

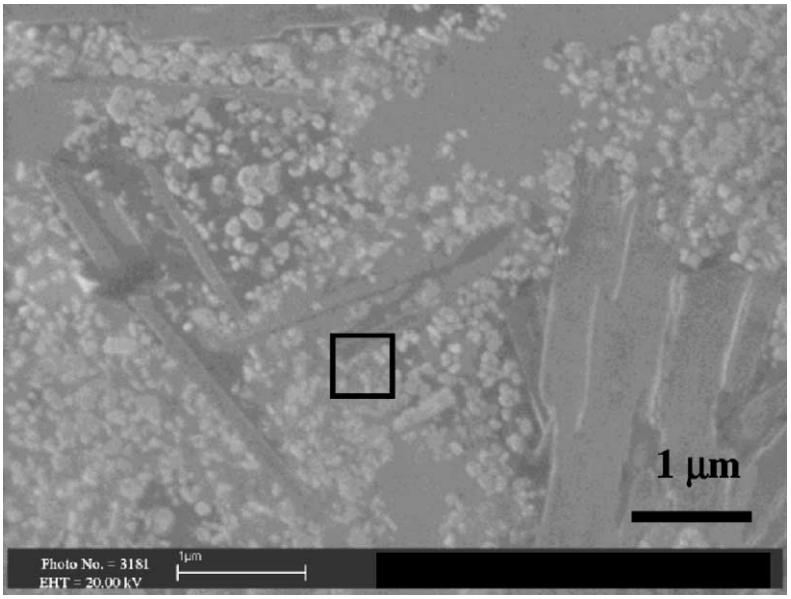

Fig. 12. SEM images collected on fractured surfaces of pellets containing 40 wt.% magnesia (detail of Fig. 11).

ing during the heating may affect its rheological property. The rheological properties of separators need to be studied to confirm these preliminary results.

4. Conclusions

Deformation tests were carried out on four different electrolyte based separators. First, we determined the appropriate amount of magnesia required in each case. We have shown that the magnesia volume fraction is a more accurate parameter than the corresponding weight fraction. Deformation master curves were obtained. Finally, by our technique, a 27–30 vol.% of magnesia was found to be enough to obtain an efficient retention whatever the electrolyte nature.

Microstructural observations of LiCl-KCl based separators were carried out. We believe that MgO enriched filamentous areas appeared during the heating step. This suggested that a solid like structure formed.

Acknowledgements

Patrick Masset gratefully acknowledges the Commissariat à l'Energie Atomique, ASB – Aerospatiale Batteries and the LEPMI for their financial support through a Ph.D. grant.

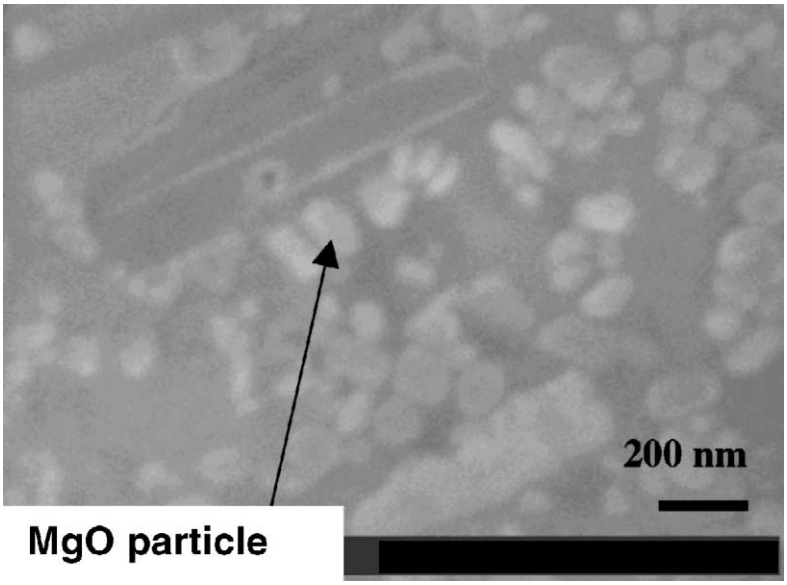

Fig. 13. SEM images collected on fractured surfaces of pellets containing 40 wt.% magnesia (detail of Fig. 14).

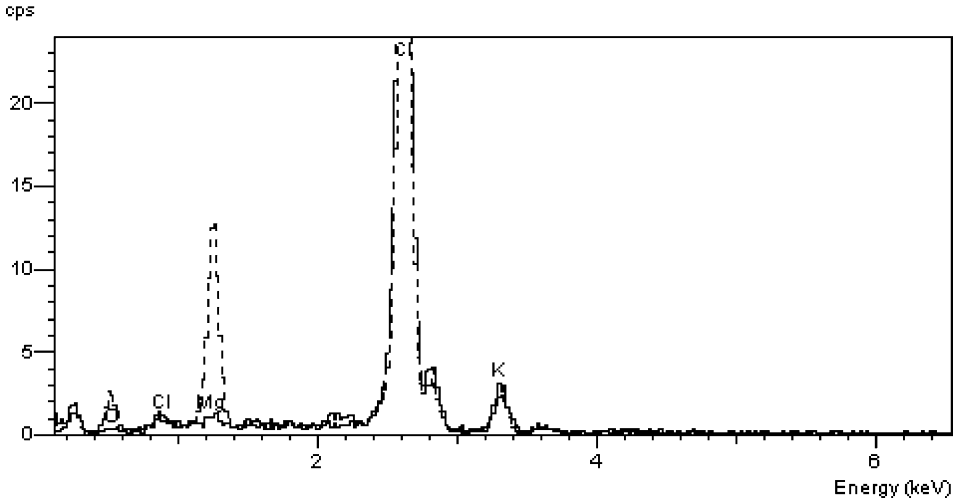

Fig. 14. EDAX analysis, LiCl-KCl (ψ_{MgO} = 40 wt.%), dashed line (- - - -) filaments, solid line (—) matrix.

Patrick Masset wishes to thank Virginie Grimal for her help during the deformation experiments.

References

[1] J.P. Mathers, C.W. Boquist, T.W. Olszanski, J. Electrochem. Soc. 125 (12) (1978) 1913.
[2] J. Schenin-King, Ph.D. thesis, Paris VI University, 1994.
[3] V.L. Cherignets, Electrochim. Acta 42 (23–24) (1997) 3619.
[4] L. Redey, M. McParland, R.A. Guidotti, Proc. 34th Int. Power Sources Conf. (1990) 128.
[5] R.A. Guidotti, F.W. Reinhardt, ECS Meeting, Philadelphia, 2002.
[6] T.D. Kaun, M.C. Hash, H. Norris, Proc. 40th Power Sources Conf. (2002) 291.
[7] R.A. Guidotti, F.W. Reinhardt, Sandia National Laboratories, SAND83-2270, 1985.
[8] R.A. Guidotti, F.W. Reinhardt, Sandia National Laboratories Report, SAND90-2318, 1995.
[9] A.G. Bergman, A.S. Arabadshan, Russ. J. Inorg. Chem. English Trans. 8 (5) (1963) 369.
[10] C.E. Johnson, E.J. Hathaway, J. Electrochem. Soc. 118 (4) (1971) 631.
[11] J. Sangster, A.D. Pelton, J. Phys. Chem. Ref. Data 16 (3) (1987) 509.
[12] R. Sridhar, C.E. Johnson, E.J. Cairns, J. Chem. Eng. Data 15 (2) (1970) 244.
[13] D.B. Leiser, O.J. Whittemore Jr., J. Am. Ceram. Soc. 50 (1) (1967) 60.
[14] E.R. Van Artsdalen, I.S. Yaffe, J. Phys. Chem. 59 (1955) 118.
[15] G.J. Janz, R.P.T. Tomkins, C.B. Allen, J.R. Downey Jr., S.K. Singer, J. Phys. Chem. Ref. Data 6 (1977) 409.
[16] R.A. Guidotti, F.W. Reinhardt, Sandia National Laboratories Report, SAND90-2103, 1991.